

Halo Concentration and the Dark Matter Power Spectrum

Kevin M. Huffenberger & Uroš Seljak

*Department of Physics, Jadwin Hall
Princeton University, Princeton, NJ 08544*

January 2003

ABSTRACT

We explore the connection between halo concentration and the dark matter power spectrum using the halo model. We fit halo model parameters to non-linear power spectra over a large range of cosmological models. We find that the non-linear evolution of the power spectrum generically prefers the concentration at non-linear mass scale to decrease with the effective slope of the linear power spectrum, in agreement with the direct analysis of the halo structure in different cosmological models. Using these analyses, we compute the predictions for non-linear power spectrum beyond the current resolution of N -body simulations. We find that the halo model predictions are generically below the analytical non-linear models, suggesting that the latter may overestimate the amount of power on small scales.

1 INTRODUCTION

In recent years, computational N -body simulations have provided important insights into the non-linear formation of structure by the dark matter. Navarro et al. (1997) (NFW) observed a ‘universal’ density profile for dark matter haloes, suggesting that the profiles depend only on the mass of the halo, with relatively little scatter between them. They also noticed that the halo concentration parameter, describing the degree of profile steepness (defined more precisely below) decreases with increasing halo mass, though the exact relation depends on the cosmology at hand. Several formulae have been suggested for this relation (Navarro et al. 1997; Bullock et al. 2001; Eke et al. 2001) which rely on fitting some mechanism to haloes culled from N -body simulations. These studies found that the concentration dependence on the power spectrum is caused primarily by the slope of the linear power spectrum. Both this and the mass dependence of concentration can be explained by the epoch of the halo formation, since less massive haloes form at higher redshift when the universe was denser and this leads to a more concentrated profile.

Another relation which appears to be universal is that of the mass function (Jenkins et al. 2001). The distribution of halo masses in N -body simulations appears to be universal in the sense that when mass is related to the fluctuation amplitude of the linear power spectrum, the mass function has a universal form. This relation has also been explored in detail in recent work (Sheth & Tormen 1999; Jenkins et al. 2001; White 2001, 2002), defining precisely what is meant by the mass and confirming the universality of the mass function for a large set of cosmological models.

While the above approaches have focused on individual haloes in the simulations by counting them and exploring their structure, for many cosmological applications all that we need is the dark matter power spectrum. This can be computed from N -body simulations as well, but com-

putational limitations prevent one from exploring a large range of cosmological models or from achieving a high resolution on small scales. For this reason many fitting formulae have been developed with increasing accuracy over the years (Hamilton et al. 1991; Jain et al. 1995; Peacock & Dodds 1996; Smith et al. 2002), although these are still significantly limited on small scales by the dynamical range of simulations.

The close connection between the two descriptions has been highlighted recently with the revival of the halo model (Seljak 2000; Peacock & Smith 2000; Ma & Fry 2000; Scoccimarro et al. 2001). For a few cosmological models, it was shown that with an appropriate choice of concentration mass dependence and mass function one can use the halo model to accurately predict the non-linear dark matter power spectrum. One of the questions we explore in this paper is whether this agreement can be extended to a wider range of models and whether the trends seen in the analysis of individual haloes are confirmed also with the power spectrum analysis. There are several reasons why this is of interest: since the selection of individual haloes is somewhat subjective it is possible that those left out may be systematically different. For example, they could be less relaxed, more recently formed and so less concentrated. An opposite effect is that because the power spectrum is a pair-weighted statistic, if there is a scatter in the mass-concentration relation then pair weighting increases the mean concentration relative to the simple particle weighting.

On the other hand, if the analysis of individual haloes is in agreement with the power spectrum analysis over the range where both are reliable, then the same analysis can be extended to smaller scales which are not resolved by cosmological N -body simulations that compute the power spectrum. The reason for this is that the resolution scale for the halo structure can be extended significantly by resimulating the representative regions of the haloes with a higher resolu-

arXiv:astro-ph/0301341v1 16 Jan 2003

tion simulation zoomed on that halo. On the other hand, a power spectrum calculation requires a large simulation volume, so that the largest scales are in the linear regime, which then implies that the mass and force resolution cannot be as high as in the simulations which focus on single haloes.

This paper is structured in the following way. We summarize the halo model and give relevant background information in §2. In §3, we give our method and results. In §4, we compare our results to other models and in §5 we summarize our conclusions.

2 BACKGROUND

2.1 The Halo Model

We begin by reviewing the formalism of the halo model to compute the non-linear dark matter power spectra, following the notation in Seljak (2000). The haloes are characterized by their mass M , density profile $\rho(r, M)$, number density $n(M)$ and bias $b(M)$. N -body simulations suggest a family of density profiles:

$$\rho(r) = \frac{\rho_s}{(r/r_s)^{-\alpha}(1+r/r_s)^{3+\alpha}}, \quad (1)$$

where ρ_s is a characteristic density, r_s is the radius where the profile has an effective power law index of -2 , and $-1.5 < \alpha < -1$ (Navarro et al. 1997; Moore et al. 1998). Here we use $\alpha = -1$, since power spectra are not sensitive to the inner parts of the halo.

As is conventional, we re-parametrize ρ_s and r_s in equation (1) in terms of a halo mass and concentration. We define the virial radius r_{vir} of a halo to be the radius of a sphere with some characteristic mean density, discussed below. Insisting that the mass contained inside r_{vir} is M fixes ρ_s for a given r_s . We introduce the concentration parameter, the ratio $c \equiv r_{\text{vir}}/r_s$. There are several definitions of virial radius used in the literature. In this paper, the virial radius is defined as the radius of a halo-centred sphere which has a mean density 180 times the mean density of the universe. This may be denoted $r_{180\Omega}$. Other authors set r_{vir} to the radius inside which the mean density is 200 times the critical density (r_{200}), a measure independent of Ω (Navarro et al. 1997, for example). Still others use a spherical collapse model to estimate the radius of a virialized halo (r_Δ). These lead to different concentrations and masses. For $\Omega = 0.3$ and $\Lambda = 0.7$, $r_{200} < r_\Delta < r_{180\Omega}$, so for the same halo with $c_{180\Omega} = 10$ one has $c_{200} \sim 6$, $c_\Delta \sim 8$, $M_{200}/M_{180\Omega} \sim 0.72$ and $M_\Delta/M_{180\Omega} \sim 0.87$. Assuming the NFW halo profile it is straightforward to translate values for concentrations and masses between these conventions. We choose $c_{180\Omega}$ as it permits the use of the universal mass function (White 2002). To avoid cumbersome notation, in this paper we refer to $c_{180\Omega}$ as c and $M_{180\Omega}$ as M .

For the mass dependence of concentration we choose a power law parametrization

$$c = c_0 (M/M_*)^\beta, \quad (2)$$

where c_0 and β are free parameters, and M_* is the non-linear mass scale, which we will define shortly. This is of course not the most general parametrization, but as we will show below it suffices for the current dynamical range.

The halo number density is written in terms of the multiplicity function via

$$n(M) dM = \frac{\bar{\rho}}{M} f(\nu) d\nu, \quad (3)$$

where $\bar{\rho}$ is the mean matter density of the universe and mass is written in terms of peak height

$$\nu \equiv \left(\frac{\delta_c(z)}{\sigma(M)} \right)^2, \quad (4)$$

where $\delta_c(z)$ is the spherical over-density which collapses at z ($\delta_c \approx 1.68$) and $\sigma(M)$ is the rms fluctuation in the matter density smoothed on a scale $R = (3M/4\pi\bar{\rho})^{1/3}$. $\nu(M_*) = 1$ defines the non-linear mass scale. A cosmology with $\Omega_0 = 0.3$, $\Lambda = 0.7$, $\Gamma = 0.2$, and $\sigma_8 = 0.9$ has $M_* \approx 10^{13} h^{-1} M_\odot$.

The power spectrum has two terms. The first corresponds to correlations in density between pairs of points where each member of the pair lies in a different halo, and so is named the ‘‘halo-halo’’ (hh) term. The second corresponds to correlations between pairs in the same halo, and is known as the one-halo or Poisson (P) term. For convenience in calculating convolutions, we work in Fourier space, introducing the Fourier transform of the halo profile, normalized by the virial mass,

$$y(M, k) = \frac{1}{M} \int 4\pi r^2 \rho(r) \frac{\sin(kr)}{kr} dr. \quad (5)$$

The mass of the NFW profile is logarithmically divergent, so in order to evaluate this integral, we must impose a cutoff. This does not have to be at the virial radius, since we know that haloes are not completely truncated there. Instead, NFW profile typically continues to $2 - 3r_{\text{vir}}$. In this regime there is already some overlap between the haloes, so for the purpose of correlations one can count the same mass element in more than one halo. Thus the mass function integrated over all the haloes may even exceed the mean density of the universe (but it can also be below it, since it is not required that all the matter should be inside a halo).

The halo-halo contribution is

$$P^{hh}(k) = P_{\text{lin}}(k) \left[\int d\nu f(\nu) d\nu b(\nu) y(M(\nu), k) \right]^2, \quad (6)$$

where $b(\nu)$ is the (linear) bias of a halo of mass $M(\nu)$, for which we use the N -body fit of Sheth & Tormen (1999). Since we want this term to reproduce the linear power spectrum on large scales we impose this constraint onto the form for $b(\nu)$ (Seljak 2000). The Poisson contribution is

$$P^P(k) = \frac{1}{(2\pi)^3} \int d\nu f(\nu) \frac{M(\nu)}{\bar{\rho}} |y(M(\nu), k)|^2. \quad (7)$$

If a cutoff beyond the virial radius is used, the mass weighting should reflect the increase. The treatment of the Poisson term on large scales is only approximate. Mass and momentum conservation require that on very large scales the non-linear term should scale as k^4 , rather than as a constant implied by equation 7, so the contribution from this term on large scales is overestimated for $k \ll r_{\text{vir}}^{-1}$. This partially compensates the increase in power from the matter outside the virial radius and for this reason we chose to use r_{vir} as the radial cutoff for the halo. The halo-halo term is only approximate, since we do not include the exclusion of haloes,

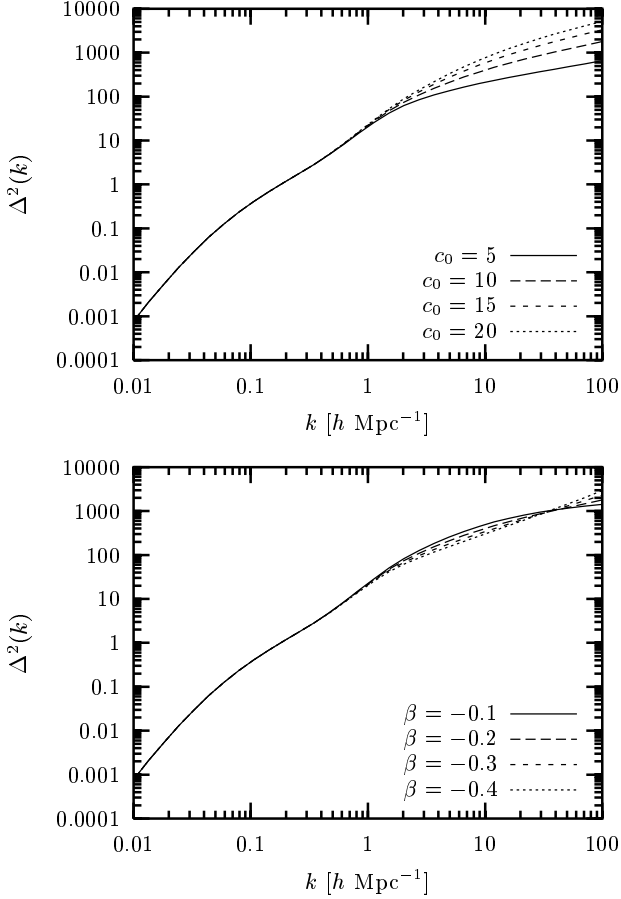


Figure 1. Using the halo model, several power spectra were generated from a cosmology with $\Omega_0 = 0.3$, $\Lambda = 0.7$, $\Gamma = 0.2$, and $\sigma_8 = 0.9$ at $z = 0$. In the upper panel, c_0 varies and $\beta = -0.2$. In the lower panel, β varies and $c_0 = 10$.

which would suppress the term. Because of these approximations one would not expect the halo model to be perfect, especially in the transition between the linear and non-linear regime.

The total power spectrum is the sum of the two contributions, $P(k) = P^{hh}(k) + P^P(k)$. On small scales, the Poisson term dominates. On larger scales, the halo-halo term dominates and reduces to the linear power spectrum. From here forward, we express the power spectrum in dimensionless form, $\Delta^2(k) = 4\pi k^3 P(k)$.

The effect on the power spectrum of varying c_0 and β in a typical Λ CDM cosmology is shown in Figure 1. The concentration controls how tightly matter is correlated within a single halo. Therefore, higher concentration means a larger one-halo term. Increasing c_0 increases the concentration at the non-linear mass, affecting the amplitude of the power spectrum where it is dominated by one-halo term.

Varying β keeping c_0 constant produces a tilt in the non-linear power spectrum around the fiducial value, which is set by the scale where the non-linear mass dominates the power spectrum contribution ($k \sim 30\text{--}40 h \text{ Mpc}^{-1}$). Haloes less massive than the non-linear mass dominate at higher k . Steeper (more negative) β means that haloes less massive than the non-linear mass will have their concentrations

enhanced, leading to an enhanced one-halo term, and more power at high k . Haloes more massive than the non-linear mass will have their concentration reduced. These dominate at intermediate k in the non-linear regime, so power there is reduced. The changes in β shown in the figure may not have much effect on the power spectrum at $k < 100 h \text{ Mpc}^{-1}$, which is the range where N -body simulations are reliable. On the other hand, they have a substantial effect on the concentration of typical-sized haloes. For the same concentration at the non-linear mass ($\sim 10^{13} h^{-1} M_\odot$), a halo at $10^{12} h^{-1} M_\odot$ has a concentration 50% lower with $\beta = -0.1$ than with $\beta = -0.4$. These masses do not dominate the power spectrum until $k > 100 h \text{ Mpc}^{-1}$, so this change does not make as much of a difference on the power spectrum at scales larger than this. This discussion suggests that while power spectrum analysis cannot provide strong constraints on the mass dependence of concentration, one can use concentration mass relation to predict the power spectrum at small scales which are not resolved by simulations.

3 METHOD AND RESULTS

We consider two sets of cases which have been extensively simulated, self-similar initial conditions and more realistic cold dark matter initial conditions. In both cases we use the fitting formulae for non-linear $\Delta^2(k)$ given by Smith et al. (2002).

3.1 Self-Similar Case

The simplest case to consider is $\Omega = 1$ Einstein-de Sitter universe with a power law linear power spectrum. In this case, β has an analytic form, provided we assume that once a halo collapses, the scale radius r_s is fixed in proper coordinates. This is suggested by the simple model which assumes the haloes remain unchanged once formed, which seems to hold in numerical simulations (Bullock et al. 2001). We follow the evolution of a single halo, as it traces out a portion of the $c(M)$ relation.

In an $\Omega = 1$ universe, density perturbations grow as the scale factor $a = 1/(1+z)$. For a power law linear spectrum, this means $P_{\text{lin}}(k) \propto a^2 k^n$. Top-hat smoothing at the scale corresponding to M yields $\sigma(M) \propto a M^{-\frac{n+3}{6}}$. For an $\Omega_m = 1$ universe, $\delta_c \approx 1.68$ is constant in time, so $\sigma(M_*)$ is also constant. This means $M_*^{\frac{n+3}{6}} \propto a$. If r_s is fixed in time, $c \propto r_{\text{vir}} \propto a$ follows from the definitions of c and r_{vir} and from $\bar{\rho} \propto a^{-3}$. Since $c \propto M_*^{-\beta}$ then $\beta \approx -\frac{n+3}{6}$ if we assume M is constant. In reality M also increases with a , which decreases β somewhat, although not by more than 20%.

We calculated halo model power spectra with $n = -2.0$ and $n = -1.5$, for which $\beta = -0.16$ and -0.25 as calculated above, with several values of c_0 . These spectra are shown in Figure 2. The agreement is quite good, given all the limitations of the halo model. At higher k in the $n = -2.0$ case, it appears that the slope of the power spectrum disagrees independent of c_0 . For $k/k_* > 2$ this model is better fit by a power spectrum with $\beta = -0.37$, $c_0 = 2.6$. However, according to figure 12 of Smith et al. (2002), simulation data do not exist for k/k_* greater than a few tens in the $n = -2$ case, so the discrepancy is not really significant.

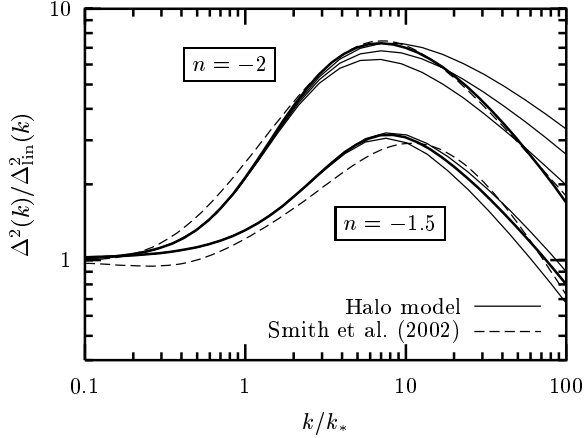


Figure 2. Non-linear power spectra in scale free models, divided by the linear power. The power law linear spectra are $\Delta_{\text{lin}}^2 = 4\pi k^3(k/k_*)^n$, where $n = -2$ and $n = -1.5$. In each case the halo model spectra for several different $c(M)$ are shown in solid lines, and the fitting formula of Smith et al. (2002) is in dashed lines. For the $n = -2$ case we show three models with $\beta = . -1667$, which is the analytically predicted value from the text. These have $c_0 = 3, 4, 5$ in increasing amplitude, and fit poorly. We also show the best-fitting $\beta = -.037$, $c_0 = 2.6$ with a thicker line. For $n = -1.5$, we show the predicted $\beta = -.25$ with $c_0 = 6, 8$, and the best-fitting $\beta = -.245$, $c_0 = 7.1$.

In the $n = -1.5$ case, which is tested against simulations to $k/k_* = 100$, the predicted $\beta = -0.25$ is close to the best fitted value. This agreement therefore confirms the assumption that haloes have a fixed scale radius once they formed.

3.2 Cold Dark Matter Models

Next we consider several flat CDM models (we do not consider open or closed models here, since they are observationally disfavored). To compare the halo model power spectrum to the Smith et al. (2002) power spectrum, we use a simple χ^2 statistic:

$$\chi^2 = \sum_{i=1}^N \left(\frac{\Delta_{\text{Smith}}^2(k_i) - \Delta^2(k_i)}{\sigma_i} \right)^2. \quad (8)$$

We distributed the $N = 40$ sample k_i evenly in $\log k$, considering $0.01 < k < 40 h \text{ Mpc}^{-1}$. This range takes us from the linear regime to some of the highest k that the fitting formula has been tested with, according to figure 16 of Smith et al. (2002). For the errors σ_i , we take 30% of the Smith et al. (2002) power. This is somewhat arbitrary, but roughly the size of the combined error in the mildly non-linear regime, and is probably conservatively large in the fully non-linear regime where the Poisson term dominates. We are ignoring the correlations between the points, so the actual value of χ^2 is just a qualitative measure of the goodness of fit.

For a variety of cosmologies, we minimized χ^2 over the two-dimensional parameter space of c_0 and β from equation (2). We employed a Powell minimization as described in Press et al. (1992) to give a best-fitting c_0 and β . All runs were given the same initial point: $c_0 = 10$ and $\beta = -0.2$, and terminated when the the minimum changed by less than

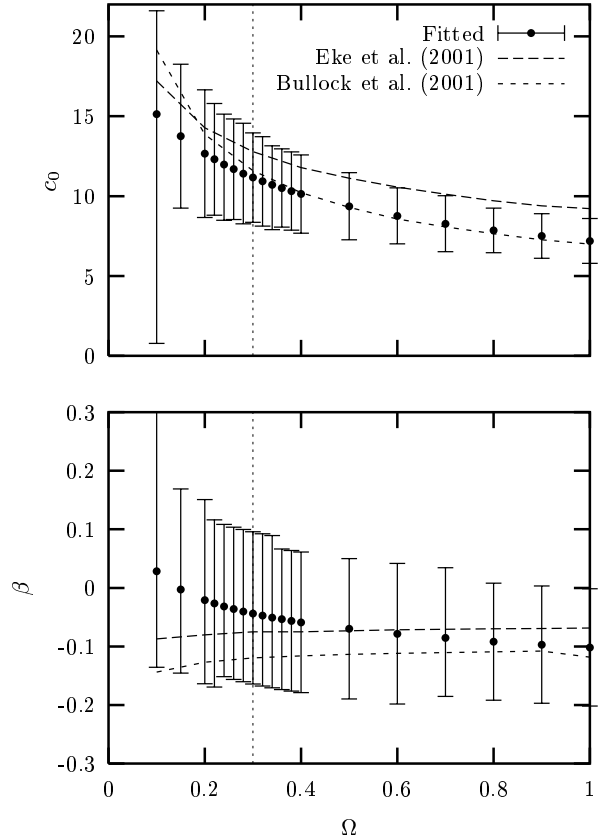


Figure 3. The values of c_0 and β at several values of the mass density parameter Ω_0 for the fitted halo model power spectrum and the models compared in §4. The vertical line denotes the fiducial model with $\Omega_0 = 0.3$. The other cosmological parameters are given in §3.2.

0.1%. We place an error bar on each minimization by calculating χ^2 on a grid about the minimum point. We compute an error contour where $\exp(-\chi^2/2)$ falls to half-maximum. The error bars in c_0 and β show the maximum extent of this contour in each direction. With this definition, these error bars cannot properly be used to set confidence limits or rule out models, but are included simply to gauge in which cosmologies parameters are better or worse constrained and to explore parameter degeneracies. Indeed, because of the range of k we consider, c_0 and β are somewhat degenerate: making β more negative has a similar effect to lowering c_0 (compare Figure 1).

We varied one cosmological parameter at a time, choosing the other parameters from a fiducial model with $\Omega_0 = 0.3$, $\Omega_0 + \Lambda = 1$, $\Gamma = 0.2$, $\sigma_8 = 0.9$, and $z = 0$. We examined the ranges $0.1 < \Omega_0 < 1.0$, $0.1 < \Gamma < 0.4$, $0.6 < \sigma_8 < 1.5$, and $0 < z < 1$. We plot the variation of c_0 and β with Ω_0 with solid lines in Figure 3. The dashed lines are discussed in §4. The relation for c_0 is well fit by:

$$c_0(\Omega_0) = 11(\Omega_0/0.3)^{-0.35}, \quad (9)$$

while β is consistent with being constant around zero or slightly negative. Note that the Ω dependence depends on

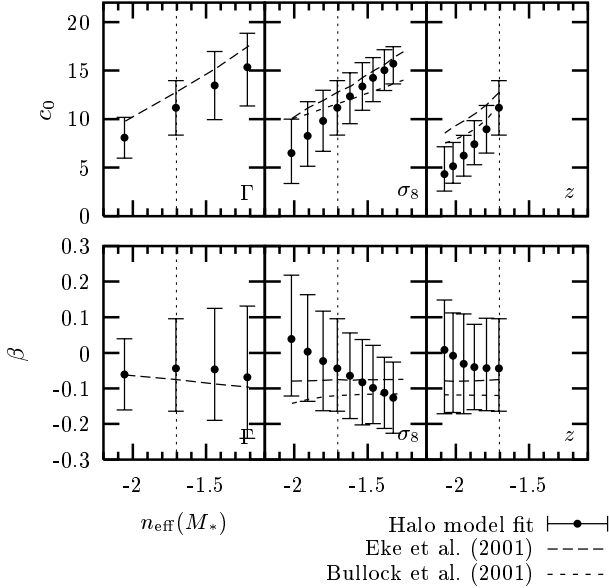


Figure 4. The values of c_0 and β as a function of the effective spectral index at the non-linear scale n_{eff} for the fitted halo model power spectrum and for the models compared in §4. The line type indicates which model. We vary one parameter at a time. The fiducial model, given in §3.2, is marked the vertical line at $n_{\text{eff}} \approx -1.7$. Each parameter increases as n_{eff} increases except for z , which decreases. In their respective panels, the points (left to right) correspond to: $\Gamma = 0.1, 0.2, 0.3, 0.4$, $\sigma_8 = 0.6, 0.7, 0.8, 0.9, 1.0, 1.1, 1.2, 1.3, 1.4$, and $z = 1.0, 0.8, 0.6, 0.4, 0.2, 0.0$.

the definition of the virial radius and with a different definition there would be a different Ω dependence.

Although c_0 and β vary with all of the other cosmological parameters, it is more instructive to present its variation with the effective power law index of the linear power spectrum at the non-linear scale,

$$n_{\text{eff}} = \left. \frac{d(\log P_{\text{lin}}(k))}{d(\log k)} \right|_{k_*}, \quad (10)$$

where $\Delta_{\text{lin}}^2(k_*) = 1$ defines the non-linear scale. The reason is that the slope of the linear power spectrum determines the epoch of formation of small haloes that merge into the larger halo. For lower effective slope n_{eff} these haloes formed later, when the density of the universe was smaller, and the final halo concentration of the larger halo is also lower. This is depicted with solid lines in Figure 4. Our fiducial cosmology has $n_{\text{eff}} \approx -1.7$. Varying Ω_0 has no effect on n_{eff} . When varying z , a portion of the variation of c_0 and β should be due to the change in $\Omega(z)$. The variation of c_0 with n_{eff} is consistent with

$$c_0 = 11(\Omega(z)/0.3)^{-0.35} \left(\frac{n_{\text{eff}}}{-1.7} \right)^{-1.6}, \quad (11)$$

while β has large errors, but is typically slightly negative.

4 COMPARISON TO HALO ANALYSIS

We now compare our results to the models of Eke et al. (2001) and Bullock et al. (2001). These are designed to re-

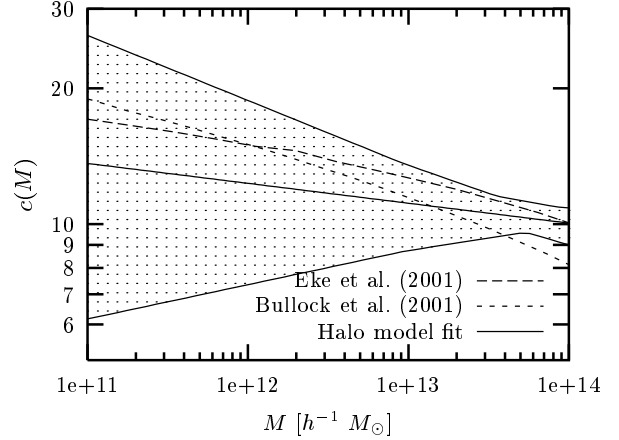


Figure 5. A comparison of the variation of the concentration parameter with mass for our fiducial Λ CDM cosmology (§3.2). The masses and concentrations here have been translated to a common virial radius convention, discussed in the text. The shaded region covers power law models within our error contour, discussed in the text, and should not be considered a limit on $c(M)$ relations of arbitrary shape.

produce the concentrations of haloes found in N -body simulations. Throughout we translate to our virial convention.

We begin by considering concentration as a function of halo mass for the fiducial Λ CDM cosmology defined in §3.2. This is plotted in Figure 5. It is clear that our results are in agreement with those from direct halo structure analysis. However, most of the information in our model comes from the haloes with masses between 10^{13} and $10^{14} h^{-1} M_{\odot}$, because haloes smaller than this dominate at scales smaller than the range we considered for our fit. This means we have a relatively short lever arm with which to determine the mass concentration relation and consequently we are unable to strongly constrain the slope β . In direct analysis of haloes, concentration is a decreasing function of mass, so $\beta < 0$. Our best fitted values for β are also typically negative, although the errors are large and positive values also cannot be excluded. The strongest confirmation of this prediction comes from the analysis of scale-free models in previous section, where β is negative for $n = -1.5$. It is clear that measuring the mass-concentration directly is a better way to determine the mass dependence of concentration rather than using the power spectrum, particularly at lower masses.

Since determining mass dependence of concentration from the power spectrum does not appear promising let us ask the opposite question: how well can we predict the power spectrum using the mass concentration relations measured directly from the analysis of individual haloes in the simulations? Figure 6 shows the power spectra calculated with power law approximations to the $c(M)$ functions shown in Figure 5, as well as the Smith et al. (2002) power spectrum. While there is good agreement between them for $k < 40 h \text{Mpc}^{-1}$, the halo models always predicts less power at $k > 40 h \text{Mpc}^{-1}$ compared to the fits to the power spectrum. However, the direct fits are not reliable in this regime, since the N -body simulations become unreliable for $k > 40 h \text{Mpc}^{-1}$, which is why the fits presented above only use information from $k < 40 h \text{Mpc}^{-1}$.

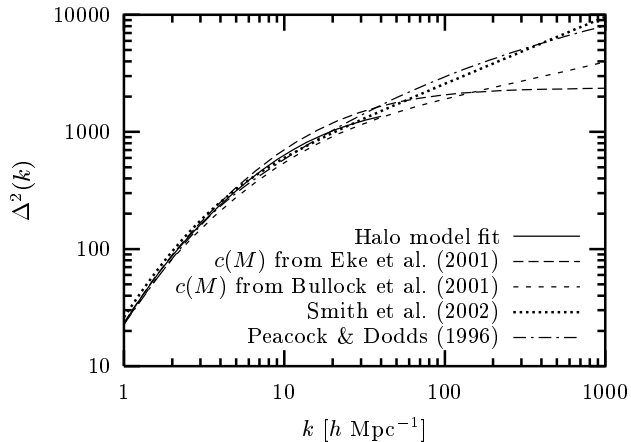


Figure 6. A comparison of power spectra generated with different $c(M)$ with analytic fitting formulae. Note that we only fit up to $k = 40 h \text{ Mpc}^{-1}$.

The conclusion from the above comparison is that on small scales there is disagreement between analytic formulae for non-linear power spectrum and the halo model. Since the analytic models have not been calibrated with simulations in this regime it is possible that they are unreliable and so the halo model should be used instead (indeed, the analytic models of Smith et al. 2002 do not even predict the power spectrum for $k > 100 h \text{ Mpc}^{-1}$). Nevertheless, since non-linear predictions at high k have been used in the literature, especially for predicting the lensing effects on small scales (e.g. Metcalf 1999), it is important to recognize their possible limitations when using them outside the regime of applicability.

It is unlikely that the discrepancy can be resolved by modifying the mass function. The existing simulations resolve the mass function down to $10^{11} M_{\odot}$, which is the mass that dominates the power spectrum at $k \sim 1000 h \text{ Mpc}^{-1}$. Substructure could boost the amount of power, since in the mass function one counts only isolated haloes, not those that are within larger haloes. Subhaloes within haloes contribute to the clustering in the same way as isolated haloes on scales that are comparable to the scale radius. However, the abundance of subhaloes is small compared to the abundance of isolated haloes even at small halo masses, so it is unlikely that this is a significant correction (Bullock et al. 2001). Similarly, while the scatter in the mass concentration relation boosts the amount of power, we find the effect is relatively small for the scatter suggested from simulations (Bullock et al. 2001; Cooray & Hu 2001) and again cannot resolve the discrepancy.

For c_0 versus Ω_0 and n_{eff} our fit to Smith et al. (2002) produces very similar trends to that in Eke et al. (2001) and Bullock et al. (2001). This comparison should be reliable, since the haloes that dominate are around $10^{13} - 10^{14} M_{\odot}$, which are abundant and well resolved in the simulations. For β we also find broad agreement, although the errors from the power spectrum method are very large.

5 CONCLUSIONS

We have used the halo model and the non-linear evolution of dark matter power spectrum (as given by the fitting formula of Smith et al. 2002) to probe the dependence of halo concentration on cosmological parameters. The most important parameters for the concentration are the matter density and the effective slope of the linear power spectrum at the non-linear scale. We present analytical expressions which give concentration at the non-linear scale as a function of these two parameters.

We examined our result against the models for halo concentration of Eke et al. (2001) and Bullock et al. (2001). We found broad agreement with the trends presented there in that we also find that spectra with lower effective slope n_{eff} have lower concentration at the non-linear mass. Although there is some difference in the mass-concentration dependence between Eke et al. (2001) and Bullock et al. (2001), we find no compelling reason to prefer one model to the other based on the power spectrum. This is because the dynamic range covered by the power spectrum analysis is too narrow to obtain a reliable mass dependence of the concentration over a wide range of masses. We have found that using these models to predict the non-linear power spectrum results in a significantly lower power spectrum on small scales compared to Peacock & Dodds (1996) and Smith et al. (2002). This suggests that care must be exercised when using these models in the range where they have not been calibrated and may indicate that the amount of dark matter power on small scales is smaller than predictions from these models.

For mildly non-linear k , even the best fitted halo models show discrepancies from the Smith et al. (2002) power spectrum at the 20-30% level, both for the self-similar and CDM models. Some of this discrepancy arises from the fits in Smith et al. (2002), which are only accurate at 10% level. However, direct comparison of the halo model to the N -body simulations of Jenkins et al. (1998) also reveals discrepancies at the similar level. This is not surprising given the approximate nature of the halo model and argues that it cannot be a full replacement for N -body simulations in the era of high precision cosmology. However, using the parameters derived in this paper, the halo model can be used for qualitative predictions of the dark matter power spectrum over much wider range of models and scales than previously available.

ACKNOWLEDGMENTS

We thank J. Bullock, V. Eke, J. A. Peacock and R. E. Smith for making their codes available. KH is supported by an NSF Graduate Research Fellowship. US is supported by NASA, NSF, Sloan and Packard Foundations.

REFERENCES

- Bullock J. S., Kolatt T. S., Sigad Y., Somerville R. S., Kravtsov A. V., Klypin A. A., Primack J. R., Dekel A., 2001, MNRAS, 321, 559
- Cooray A., Hu W., 2001, ApJ, 554, 56
- Eke V. R., Navarro J. F., Steinmetz M., 2001, ApJ, 554, 114

- Hamilton A. J. S., Matthews A., Kumar P., Lu E., 1991, ApJ, 374, L1
- Jain B., Mo H. J., White S. D. M., 1995, MNRAS, 276, L25
- Jenkins A. et al., 1998, ApJ, 499, 20
- Jenkins A., Frenk C. S., White S. D. M., Colberg J. M., Cole S., Evrard A. E., Couchman H. M. P., Yoshida N., 2001, MNRAS, 321, 372
- Ma C., Fry J. N., 2000, ApJ, 543, 503
- Metcalf R. B., 1999, MNRAS, 305, 746
- Moore B., Governato F., Quinn T., Stadel J., Lake G., 1998, ApJ, 499, L5
- Navarro J. F., Frenk C. S., White S. D. M., 1997, ApJ, 490, 493
- Peacock J. A., Dodds S. J., 1996, MNRAS, 280, L19
- Peacock J. A., Smith R. E., 2000, MNRAS, 318, 1144
- Press W. H., Teukolsky S. A., Vetterling W. T., Flannery B. P., 1992, Numerical recipes in FORTRAN. The art of scientific computing. Cambridge: University Press, —c1992, 2nd ed.
- Scoccimarro R., Sheth R. K., Hui L., Jain B., 2001, ApJ, 546, 20
- Seljak U., 2000, MNRAS, 318, 203
- Sheth R. K., Tormen G., 1999, MNRAS, 308, 119
- Smith R. E. et al., 2002, in astro-ph/0207664
- White M., 2001, A&A, 367, 27
- White M., 2002, in astro-ph/0207185, to appear in ApJS.